Time of Nucleation of Phase-Slip Centers in $YBa_2Cu_3O_7$ Superconducting Bridges

F. S. Jelila, J-P Maneval,* F-R Ladan, F. Chibane,† and A. Marie-de-Ficquelmont
Département de Physique, Ecole Normale Supérieure, 24 rue Lhomond, 75231, Paris 5, France

L. Méchin and J-C Villégier
Commissariat à l'Energie Atomique, DRFMC-SPSMS, 38054, Grenoble 9, France

M. Aprili and J. Lesueur
CSNSM, Bâtiment 108, Université Paris-Sud, 91045, Orsay, France
(Received 5 December 1997)

Narrow $YBa_2Cu_3O_7$ films, excited by pulses of supercritical current, had their nanosecond electric response monitored in zero applied magnetic field. Delayed voltage steps plus constant differential resistance, characteristic of phase-slip centers (PSC), are observed at all temperatures. The duration of the initial zero voltage state is well fit by Ginzburg-Landau based theories, with a gap relaxation time controlled by phonon escape. At higher levels of excitation, PSC's give birth to slowly spreading normal hot spots. [S0031-9007(98)06897-5]

PACS numbers: 74.76.Bz, 74.25.Kc, 74.40.+k, 74.50.+r

Superconductivity is perturbed, not suppressed, by a critical current. Thanks to vortex motion, the growing phase differences of the order parameter wave function relax by multiples of 2π [1], a process which allows the material to preserve long range order while sustaining a voltage. In filamentary structures, similar quantum phase jumps occur in short, fixed, zones named phase-slip centers [2] (PSC). So, dissipation arises in a way fundamentally different from a transition into the normal state. A second singular feature is the long persistence of the zero voltage state after the application of the supercritical current, much beyond the natural (picosecond) time h/Δ (Planck constant divided by the energy gap). Pals and Wolter [3] discovered this delay, or PSC nucleation time, t_d on aluminum film strips. Interpreting it as the time required to achieve complete collapse of the order parameter, and using a time-dependent Ginzburg-Landau (TDGL) equation based on the nonequilibrium energy-mode gap relaxation time [4], they could account fairly for their experimental data.

It would be difficult to make any predictions for cuprate superconductors, due to their utterly short coherence length. Nevertheless, the dc current-voltage (I-V) curves of high-T_c narrow bridges indeed display the steps and the expected response to microwave radiation [5] related to PSC's. This Letter reports on the first observation of the delay t_d in epitaxial $YBa_2Cu_3O_7$ thin films, and its interpretation through TDGL. At the same time, we tackle directly the troublesome problem of heating in a dissipative center.

Our experiments were performed in zero applied magnetic field on c-axis textured films with typical misorientation 0.5 degree of arc. Sample LL-109N is a 75 nm thick film evaporated [6] on [100] MgO with cationic composition $YBa_{1.88}Cu_{3.04}$. Our bridge has resistivity $\rho(300\text{ K}) = 350\ \mu\Omega$ cm, a ratio RRR $= \rho(300\text{ K})/\rho(100\text{ K}) = 2.8$, and a critical temperature $T_c = 89$ K. Samples TO-34 and TO-S35, obtained by dc hollow cathode sputtering [6], had similar electrical characteristics. Finally, sample LZCYB77 is a 35 nm thick film deposited by laser ablation [6] on [100] Si covered with a buffer layer (70 nm YSZ; 10 nm CeO_2). Our bridge had $\rho(300\text{ K}) = 1.9$ mΩ cm, and RRR $= 2.6$.

According to the standard PSC model [7], each phase-slip event produces a burst of quasiparticles, whose diffusion eventually determines the length of the dissipative zone. Therefore, the ideal I-V curves beyond I_c are made up of segments of constant differential resistance dV/dI, one for each PSC, linking successive voltage steps. Figure 1 shows this for an YBCO film deposited on CeO_2 covered sapphire. Notable features are the forked ascension and the hysteretic voltage jumps of the I-V curves.

To study the response on the nanosecond scale, we used a coaxial circuit (impedance $Z_0 = 50\ \Omega$) capable of 250 ps rise time in its most compact form, fed with electrical step functions. The sample is essentially current-biased so that, in its transient zero-resistance state up to t_d, the sample carries a current $I_i = 2V_i/Z_0$, where V_i is the input voltage. However, when a voltage V develops along the bridge, the current drops to $(2V_i - V)/Z_0$, currently a correction of a few percent. As we will observe below, this may cause a net decrease of the signal, depending upon the location of the resistive singularity with respect to the probe. In any case, it was taken into account in the establishment of the I-V relationship.

Figure 2 shows an example of the wealth of phenomena achievable in this configuration. For current flowing from A to B in sample LL-109N, the critical value is $I_c = 29.0$ mA at $T_0 = 60$ K. With the sample excited by pulses of amplitude 29.7 mA, the response begins with an inductive peak preceding a flat part which is the Ohmic drop at the gold-to-YBaCuO contacts (see the two bottom

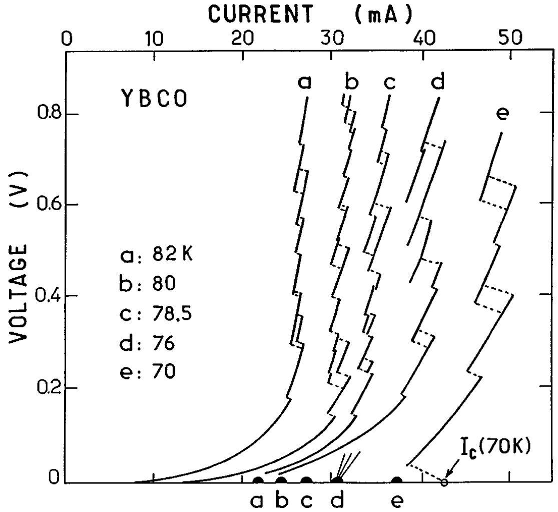

FIG. 1. dc current-voltage characteristics of bridge TO-S35 (length: 200 μm; width: 20 μm; thickness: 90 nm) at temperatures noted a, b, c, d, and e, showing the resistance jumps at each critical current. Note that all segments of constant dV/dI on a curve seem to originate from a single point on the $V = 0$ axis (points also indexed a, b, c, d, and e).

curves of Fig. 2). Then comes a voltage jump, common to probes A and C, at time marked t_{d1}. In the absence of such a voltage at probe D (not shown), one is led to locate the dissipation between the geometrical points C' and D'. We call it PSC in consideration of three features: delayed signal, voltage jump rather than a smooth function of the current, and stability after a short period. (Depending upon the sample, we could record up to three PSC's within 15% excursion above I_c.)

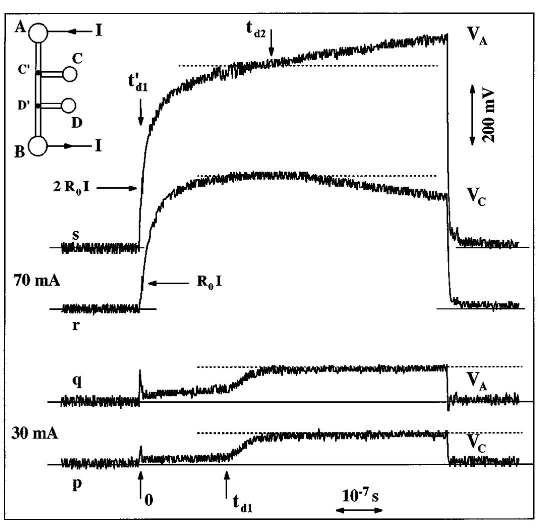

FIG. 2. (Graphs p, q, r, and s, from bottom to top). Voltage versus time across YBaCuO sample LL-109N (width: 10 μm; length: 3 mm) in response to a rectangular pulse of current at $T = 60$ K. (p, q) Signals at probes C and A for $I/I_c = 1.02$, showing the rise of a PSC at time t_{d1}. (r, s) Signals taken at the same probes for $I = 2{,}38 I_c$ showing the development of a hot spot at time t_{d2}. The symbols $R_0 I$ and $2R_0 I$ mark the amplitudes of the voltage drops at terminal contacts.

Increasing the input current causes the delay t_{d1} to shrink, until it falls to an unmeasurably small value when I exceeds about $2I_c$ (see t'_{d1} in the two top curves of Fig. 2). This general move goes along with an increase of the plateau voltage until, at a time marked t_{d2}, another structure appears, whose location between A and C' is revealed by $V_A \neq V_C$. During its development, the rising V_A is the product $R \cdot I$ of an increasing resistance by a decreasing current, while C merely monitors the decrease of $(2V_i - V_A)/Z_0$. This additional feature, expanding over a characteristic time of order 1 μs, is, we believe, a hot spot [7], to be discussed later.

At fixed temperature, t_d is a sensitive function of I especially just above $I_c(T)$, defined throughout this work as the current giving the longest observable delay, that is, 500 ns. While t_d is always well defined at low T, the voltage response becomes gradually faint at higher temperatures, with a limit of readability around 70 K. Typical data are plotted in semilog coordinates in Fig. 3.

Following Pals and Wolter, we plot on the same graph the function derived from TDGL in one dimension [3]:

$$t_d(I/I_c) = \tau \int_0^1 \frac{2f^4 df}{(4/27)(I/I_c)^2 - f^4 + f^6}, \quad (1)$$

where the adjustment constant τ is to be interpreted as an effective gap relaxation time. The dummy variable f stands for the normalized modulus of the order parameter, and the integration boundaries express that f goes from 1 to 0 within time t_d. For sample LZCYB-77, it can be seen that $\tau = 5$ ns provides asymptotic agreement for long delays. A similar fitting procedure for

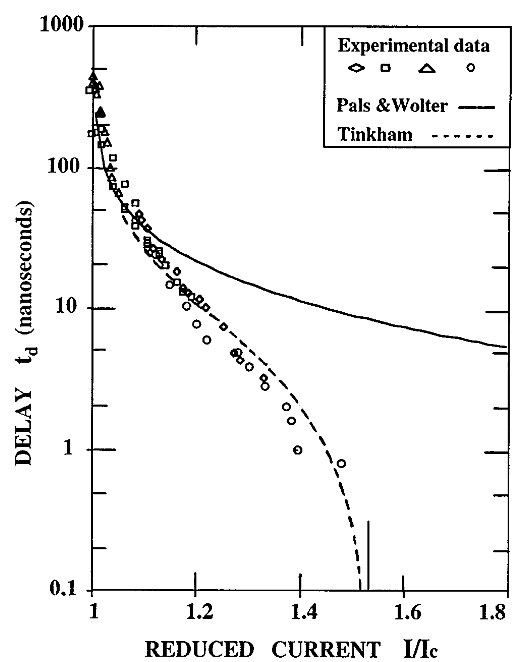

FIG. 3. Delay t_d at 4.2 K plotted as a function of I/I_c in sample LCZYB-77 (length: 50 μm; width: 10 μm; $I_c = 72$ mA). The solid curve is the function τF_{PW} of Eq. (1) drawn for $\tau = 5$ ns. Broken line derives from Eq. (2) with same τ.

samples TO-34 and LL-109N gave $\tau = 2$ ns and 6.5 ns, respectively.

The loss of validity of Eq. (1) for delays t_d of the order, or shorter than τ, was pointed out by Tinkham [8], who treated the case of arbitrarily fast gap variations. Taking Eq. (64) of Ref. [8] in the limit $T \ll T_c$ brings a formula for t_d having the same structure as Eq. (1), with the numerator of the integrand replaced by

$$2f^4 + 1.65f^5 - 0.5(I/I_c)^2. \tag{2}$$

The result of this refined calculation, assuming the same choice of τ as before (5 ns), shows a striking agreement over the whole range of currents investigated (Fig. 3, dashed curve). This is surprising in view of the parameters of our experiment, since the PSC model was designed for bridges having their transverse extension smaller than both the coherence length and the magnetic penetration depth [2,3]. However, from theory and experiment [9], it may be credited with broader validity, whenever h/Δ is significantly shorter than the inelastic collision time.

In order to capture the temperature behavior of τ, Eq. (1) suggests to determine t_d at constant values of $I/I_c(T)$ or, equivalently, to measure at each temperature the ratio $I(T, t_d)/I_c(T)$ which produces selected values of t_d (see Fig. 4 for $t_d = 50$ and 100 ns). If we reckon data dispersion as the typical uncertainty (0.5%) affecting pulse height measurements, the main information is that a given t_d requires a constant ratio I/I_c up to about 60 K, which in turn defines a *strictly T-independent prefactor* τ. As a check of accuracy, we managed to bracket the data (Fig. 4) between a couple of horizontal lines A and B defined, through Eq. (1), with two similar values of τ. (There is one such couple for each selected t_d.) To define A and B in sample LL-109N, we used, respectively, the times $\tau = 6$ and 7 ns which flank correctly the 6.5 ns used to fit t_d vs I/I_c in this sample (see *supra*).

Our τ's turn out to be orders of magnitude longer than any known quasiparticle inelastic lifetimes as soon as $T > 10$ K. We note that these are expected to vary considerably with T (proportionally to T^{-3} for the electron-phonon interaction [10]). Therefore, we believe gap relaxation is limited not by intrinsic relaxation mechanisms, but rather by the rate of phonon removal from the film, so that film cooling actually sets the pace of gap relaxation [11]. In the case of epitaxial YBCO on a crystalline substrate, several authors [12–14] have independently measured cooling times (a) proportional to film thickness and (b) independent of T practically up to T_c. Theoretically, such properties derive from the phonon radiation model, so called with reference to the optical blackbody, according to which the power transferred goes as T^4 (Stefan's law), in proportion to the lattice energy $\int CdT$, where $C = \beta T^3$ is the Debye specific heat. In that way, τ in Eq. (1) should be identified with the phonon escape time τ_γ.

The results of the present work ($\tau = 6.5$ and 2 ns, respectively, for 75 and 30 nm films) compare very well with determinations of τ_γ based on the decay of photoinduced resistance in similar YBCO-on-MgO films (4 ns for a 48 nm film [12] up to 81 K; 2.4 ns for a 30 nm film [14] throughout the range 1.3 to 50 K). Sample LZCYB-77 (35 nm), with a comparatively large $\tau = 5$ ns, is no contradiction since it comprises two matching layers between film and substrate.

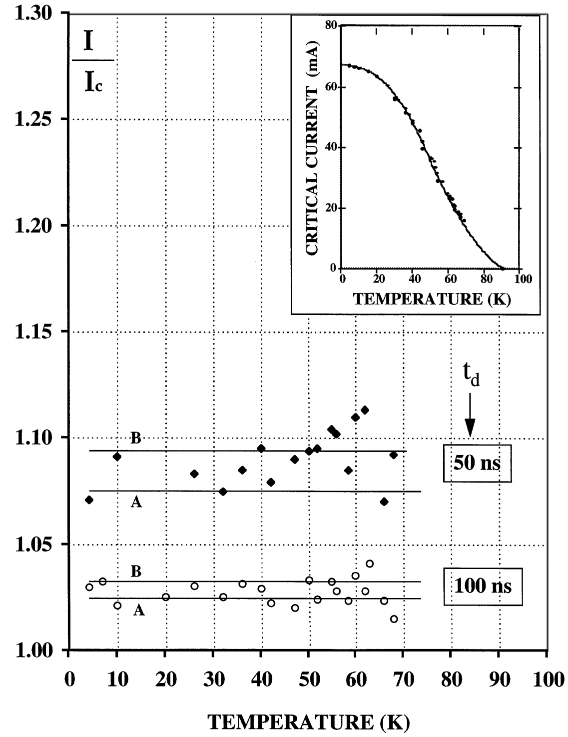

FIG. 4. Properties of bridge LL-109N in the range 4.2 to 68 K, for current flowing between probes A and D (see inset of Fig. 2). Plot of the ratios $I(T, t_d)/I_c(T)$, where $I(T, t_d)$ is the current producing a voltage jump at time t_d. Here, $t_d = 50$ ns and $t_d = 100$ ns. For lines A and B, see text. Inset: Critical current I_c versus T. From 0 to 50 K, the fitting curve is $I_c = I_{c0}\,[1 - a\theta - b\theta^{5/2}]$, with $\theta = T/92$ K, $I_{c0} = 67.5$ mA, $a = 0.1$, and $b = 0.077$. From 50 to 70 K, we took $I_c = I^*[1 - \theta]^{3/2}$ with $I^* = 121$ mA.

The constant differential resistance dV/dI observed in the dc characteristics (Fig. 1) also shows systematically in the pulse mode (Fig. 5). An important quantity is I_0, defined by $V = (dV/dI)(I - I_0)$, which represents the time-averaged superconducting fraction [2] traversing the dissipative structure for total current I. The ratio I_0/I_c is definitely nonzero (0.48 for sample LL-109N; 0.71 and 0.72, respectively, in TO-34 and LZCYB-77), proving that a sizable part of the current is carried as a superfluid.

On the other hand, the differential resistance (15 Ω from the graph), equivalent to about 16 μm of normal material is difficult to interpret quantitatively. If this figure is to correspond to twice the quasiparticle inelastic diffusion length [7] $(v_F \ell_e \tau_2/3)^{1/2}$ with v_F the Fermi velocity, ℓ_e the mean free path, and τ_2 an inelastic lifetime ($\tau_2 = \tau_\gamma = 6.5$ ns), it is too long by a factor of about 5. This is a severe discrepancy which might

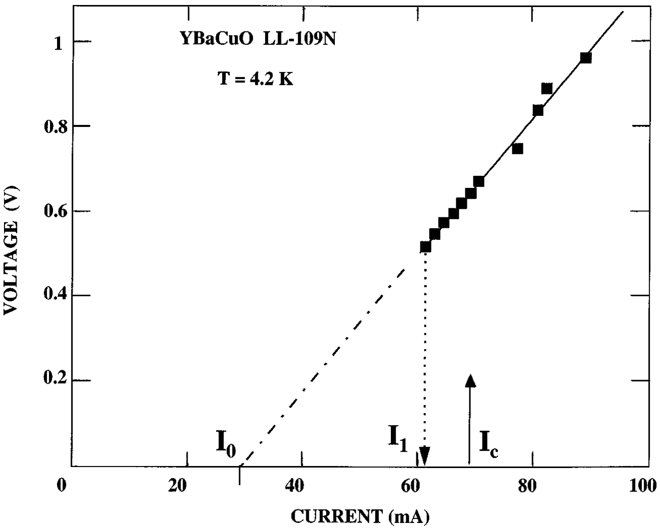

FIG. 5. Voltage on top of the first PSC plotted versus current. Critical current $I_c = 68$ mA; jump back current $I_1 = 61$ mA; $I_0 = 29$ mA, as given by extrapolation of the segment of constant slope. The differential resistance, $dV/dI = 15\ \Omega$, corresponds to 16 μm of material in the normal state.

be proper to high-T_c materials, and to their complex and imperfect crystalline structure, whereas it also reminds us that the physical origin of τ_2 and its temperature behavior have aroused a variety of interpretations [15], without prejudice to the overall PSC picture yet.

Finally, we wish to come back to the distinct signal shapes observed at low and high currents in Fig. 2. For $I = 30$ mA (graphs p and q of Fig. 2), one obtains the temperature T that would be reached in a purely resistive element by equating the Joule power per unit length $\rho I^2/wd$ to the phonon power $(1/4)\beta(T^4 - T_0^4)wd/\tau_\gamma$ radiated to the substrate. For sample LL-109N, with the parameters $w = 10\ \mu$m, $d = 75$ nm, $\tau_\gamma = 6.5$ ns, $\rho(90\text{ K}) = 115\ \mu\Omega$ cm, $\beta = 0.56$ mJ/mol K^4, molar volume: 104 cm^3, $T_0 = 60$ K, one gets $T = 68.5$ K, definitely below T_c. Further, the dissipation $\rho I^2/wd$ has to be replaced by $\rho I(I - I_0)/wd$ inside a PSC, which brings $T(\text{PSC})$ closer to 65 K.

For those signals, referred to as hot spots, observed at 70 mA in graphs r and s of Fig. 2, an equivalent calculation gives $T = 88.9$ K, at the foot of the resistive transition, even if such an accurate coincidence may be somewhat misleading. (In another experiment, we find 88.1 K for $T_0 = 56$ K and $I = 72$ mA.) Anyway, the signals emerging at t_{d2}, which we could observe over microseconds, very likely reflect the slow growth of normal ($T > T_c$) zones, in contrast to the constancy in time of PSC signals. In current-biased bridges, assumed to be homogeneous, this growth should meet no other limit than complete transition.

In summary, $YBa_2Cu_3O_7$ narrow bridges passing a overcritical current get striated by one or several stable phase-slip zones, with a nucleation time t_d well-fitted by the TDGL expression which was designed for low-T_c materials near their transition temperature. On the other hand, the intrinsic mechanisms of gap relaxation are concealed by phonon bottleneck, and are therefore unattainable.

We are indebted to B. Plaçais for stimulating discussions, and to Laboratoire de Microélectronique et Microstructures (CNRS, Bagneux) for access to their technical facilities.

*Laboratoire de Physique de la Matière Condensée, associated with Centre National de Recherche Scientifique, affiliated to Universities Paris 6 and Paris 7.

†Presently with Faculté des Sciences, University Ibnou Zohr, Agadir, Marocco.

[1] P.W. Anderson and A. Dayem, Phys. Rev. Lett. **13**, 195 (1964).
[2] T.J. Rieger, D.J. Scalapino, and J.E. Mercereau, Phys. Rev. B **6**, 1734 (1972).
[3] J.A. Pals and J. Wolter, Phys. Lett. **70A**, 150 (1979).
[4] M. Tinkham, *Introduction to Superconductivity* (McGraw-Hill, Singapore, 1996), 2nd ed., Chap. 11.
[5] V.M. Dmitriev, I.V. Zomlochevskii, and E.V. Kristenko, Physica (Amsterdam) **235–240C**, 1973 (1994).
[6] J. Lesueur *et al.*, J. Alloys Compd. **251**, 156 (1997); J-C Villégier *et al.*, Mater. Sci. Eng. **B15**, 92 (1992).
[7] W.J. Skocpol, M.R. Beasley, and M. Tinkham, J. Low Temp. Phys. **16**, 145 (1974).
[8] M. Tinkham, *Non-Equilibrium Superconductivity, Phonons and Kapitza Boundaries,* edited by K.E. Gray (Plenum, New York, 1981).
[9] A. Weber and L. Kramer, J. Low Temp. Phys. **84**, 289 (1991), and references therein.
[10] J-P Maneval, F. Chibane, and R.W. Bland, Appl. Phys. Lett. **61**, 339 (1992).
[11] Examples of such a behavior are found in the literature. See, for instance, C.C. Chi, M.M.T. Loy, and D.C. Cronemeyer, Phys. Rev. B **23**, 124 (1981).
[12] G.L. Carr *et al.*, Appl. Phys. Lett. **57**, 2725 (1990).
[13] F.A. Hegmann and J.S. Preston, Phys. Rev. B **48**, 16 023 (1993).
[14] J-P Maneval, Phan Hông Khôi, and F. Chibane, Physica (Amsterdam) **235–240C**, 3389 (1994).
[15] R. Tidecks, *Non-Equilibrium Phenomena in One-Dimensional Superconductors* (Springer-Verlag, Berlin, 1990).